

These authors calculated s -, p -, d -, and f -wave e^- -He elastic scattering phase shifts by the variational method. Their results for d -wave phase shifts were obtained *with* and *without* the inclusion of f orbitals in the basis set. Our results for d -wave phase shift are in very good agreement with their d -wave results with s , p , and d basis.

³⁰A. Temkin, Phys. Rev. **107**, 1004 (1957).

³¹R. LaBahn and J. Callaway, Phys. Rev. **180**, 91 (1969); Phys. Rev. A **2**, 366 (1969).

³²S. P. Khare and P. Shoba, J. Phys. B **4**, 208 (1971).

³³P. G. Burke, J. W. Cooper, and S. Ormande, Phys. Rev. Letters **17**, 345 (1966); Phys. Rev. **183**, 245 (1969).

³⁴P. O. Löwdin, in *Proceedings of the Robert A. Welch*

Foundation, II (Robert A. Welch Foundation, Houston, 1959). See also H. Shull and P. O. Lowdin, J. Chem. Phys. **30**, 617 (1959).

³⁵N. Cressy, K. R. Miller, and K. Ruedenberg, Int. J. Quant. Chem. **3**, 107 (1969).

³⁶G. Wendin, J. Phys. B **4**, 1080 (1971).

³⁷S. Sengupta and A. Mukerji, J. Chem. Phys. **47**, 260 (1967).

³⁸C. Moore, Atomic Energy Levels, Natl. Bur. Std. (U. S.) Circ. No. 467, (U. S. GPO, Washington, D. C., 1949), Vol. I.

³⁹T. Kinoshita, Phys. Rev. **105**, 1490 (1957).

⁴⁰W. C. Martin, J. Res. Natl. Bur. Std. (U.S.) **64**, 19 (1960).

Scattering of Light Ions in the Weakly Screened Coulomb Field of Gold Nuclei

H. H. Andersen, J. Böttiger, and H. Knudsen

Institute of Physics, University of Aarhus, DK-8000 Aarhus C, Denmark

(Received 10 July 1972)

The differential cross section for scattering of 300–2000-keV H^+ and 300–500-keV He^+ and Li^+ through 3° – 15° by gold targets has been measured. The targets were thin (34 – $220 \mu\text{g}/\text{cm}^2$), vacuum-deposited polycrystalline foils. To eliminate the influence of multiple scattering, several target thicknesses were used to allow extrapolations to zero thickness. The agreement between our experimental data, theoretical predictions, and published experimental data is found to be satisfactory.

I. INTRODUCTION

Elastic scattering of ions on atoms yields information on the screening of the Coulomb interaction by the electrons surrounding the partners in the collision and is thus of interest for theoreticians as well as for experimentalists. While it is fairly straightforward to calculate the electron distribution of a single atom from a statistical model,¹ the description of the electron distribution of two colliding atoms is more complicated. For close collisions, interaction by an exponentially screened Coulomb potential² is found to work rather well, but this interaction potential falls off much too rapidly with distance. A Thomas-Fermi (TF) calculation may then be attempted also for the two-atom case.

In a comprehensive paper, Lindhard *et al.*³ showed that the similarity properties of atoms in the TF model, together with some simple assumptions, allowed a very simplified expression for the differential cross section. They expressed the cross section as being a function of one single parameter proportional to the product of projectile energy and recoil energy in the collision. If, further, these energies are expressed in dimensionless TF energy units, it is necessary to calculate only a single universal function numerically. By means of a simple procedure, this function may then be used to find differential cross sections for all com-

binations of projectiles, targets, projectile energies, and scattering angles.

The experimental verification of the above-mentioned predictions has not been very extensive. Loftager *et al.*⁴ investigated mainly the region of larger impact parameters corresponding to scattering in strongly screened fields. Other investigators^{5,6} obtained a large number of experimental data that may be directly compared to those of the present paper, but these data were not analyzed to test the scaling properties, nor were they compared in absolute magnitude with the TF cross section.

Thus, there appears to be a need to investigate experimentally the results of Lindhard *et al.*³, not only for the intrinsic interest in interaction potentials, but also because the weakly screened cross sections are important for further progress, for example, in the calculation of phenomena involving recoil energies of target atoms. Recent examples are calculations of sputtering yields⁷ and radiation damage.⁸

The present experiments have been made partly for the above-mentioned purposes, partly for the purpose of examining the possibilities of using solid targets for measurements of scattering cross sections at relatively large impact parameters (see also Ref. 5). 300–2000-keV H^+ and 300–500-keV He^+ and Li^+ ions scattered through 3° – 15° in the laboratory system were used. The targets

were thin ($34\text{--}220\ \mu\text{g}/\text{cm}^2$) self-supporting polycrystalline gold foils and scattering cross sections were obtained by extrapolating results from many targets to zero thickness. Relative cross sections were measured by means of a fixed and a movable solid-state detector, the former acting merely as a beam integrator. A removable Faraday cup was used to calibrate the fixed counter for different projectiles and projectile energies. Absolute values of the cross sections may be determined from the measurements if one of the cross sections in question is known. As such a reference point we chose scattering of 1.5-MeV H^+ through 15° , which is very close to pure Rutherford scattering.

II. EXPERIMENTAL

The experimental equipment is identical to that used previously for investigation of multiple scattering of heavy ions in thin carbon⁹ and gold¹⁰ films. In Ref. 9, the setup is described in detail, and only a brief discussion will be given here. Figure 1 shows a schematic representation of the equipment. The direction of the incident beam from either a 600-kV heavy-ion accelerator or from a 2-MV Van de Graaff is accurately defined by means of two collimators. Particles scattered in the target are detected by conventional solid-state surface-barrier detectors N and T , of which N is fixed, spans a large solid angle, and is used for normalization, while T may be moved in two directions, each perpendicular to one another. A small aperture accurately defines the scattering angle. The average scattering angle of the detected particles can be determined to better than 0.05° .

The targets are evaporated, $34\text{--}200\text{-}\mu\text{g}/\text{cm}^2$ -thick polycrystalline gold films with a 3-mm-diam self-supporting part. They have a slight $\langle 111 \rangle$ texture. The $\langle 111 \rangle$ direction is not one of the most open channels in the fcc lattice, and channeling will not influence the single-scattering yield. A further discussion of the targets will be found in Ref. 10.

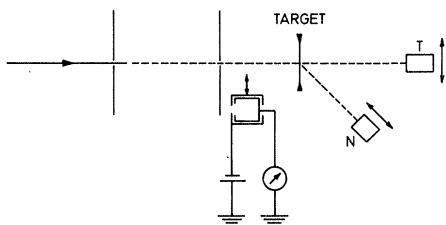


FIG. 1. Schematic diagram of experimental setup. The Faraday cup may be inserted into the beam for normalization of the solid-state counters N and T . Counter N is at a fixed angle, but the distance to the target is adjustable so as to obtain a convenient counting rate. Counter T may be scanned across the scattered beam and is directly used for measurements of cross sections.

For a given projectile and projectile energy, we need to use only N and T to obtain relative cross sections. To be able also to compare different projectiles and energies, a normalization of N is necessary. This normalization is performed by means of a removable Faraday cup inserted in front of the target. Alternatingly, the current and the yield are measured. Through the normalization of N , we may then obtain the yield per incident particle in the movable detector T . As the solid angle subtended by T is precisely known,⁹ the equipment allows us to measure cross sections if the thickness is known or vice versa. As discussed and checked in detail in Ref. 9, the absolute accuracy of the current measurement is considered to be better than 2%, and the thickness determinations to be better than 5%. As the measurements of cross sections for one projectile relative to another involves the same procedure as a thickness determination, these relative cross sections may also be measured to better than 5%.

The cross section for the scattering of 1.5-MeV protons through 15° (the reference point) is assumed known in order to convert relative into absolute cross sections. The calculated cross section for this event is approximately 2% below the Rutherford cross section. The uncertainty in this value is negligible in this connection. Furthermore, it must be assumed that the yield at the reference scattering point is unaffected by multiple scattering. This seems reasonable, the scattering angle being approximately 25 times larger than the half-width of the multiple-scattering distribution for the thickest foil at the energy involved. The noninfluence of multiple scattering is also seen by comparing scattering yields for foils of different thicknesses, as described below.

At the 600-kV machine, it is not possible to reach a reference point where the scattering yield is uninfluenced by multiple scattering. Thus, multiple-scattering corrections obtained at the Van de Graaff were used at the 600-kV accelerator. For 500-keV protons scattered through 15° , this correction is found to be 12% of the scattering yield for the thickest target. These corrections must also be applied to the thicknesses in our multiple-scattering measurements,¹⁰ where the relative correction is proportional to the stated thickness and amounts to the above-mentioned 12% for the $220\text{-}\mu\text{g}/\text{cm}^2$ foil. For carbon,⁹ these corrections to the thickness measurements are entirely negligible.

III. THEORY

Lindhard *et al.*³ showed that to a good approximation, the classical differential cross section for elastic scattering may be written as a function of projectile energy E times recoil energy. As

the recoil energy is proportional to $E \sin^2 \frac{1}{2}\vartheta$, where ϑ is the center-of-mass scattering angle, this means that the important parameter will be

$$t = \epsilon^2 \sin^2 \frac{1}{2}\vartheta. \quad (1)$$

Here the energy is expressed in the dimensionless TF energy units defined by

$$\epsilon = \frac{M_1 M_2 v^2 a}{2(M_1 + M_2) Z_1 Z_2 e^2}. \quad (2)$$

M_1 , Z_1 and M_2 , Z_2 are masses and atomic numbers of projectiles and target atoms, respectively; v is the velocity of the incident ions and the screening radius,

$$a = a_0 \times 0.885 (Z_1^{2/3} + Z_2^{2/3})^{-1/2}, \quad (3)$$

where a_0 is the first Bohr radius of the hydrogen atom.

In terms of parameter t as defined by Eq. (1), Lindhard *et al.*³ showed that the cross section could be written in the form

$$d\sigma = \pi a^2 \frac{dt}{2t^{3/2}} f(t^{1/2}), \quad (4)$$

where the function $f(t^{1/2})$ was calculated numerically for the TF model, i. e., that a potential of the form

$$V(r) = Z_1 Z_2 (e^2/r) \varphi_0(r/a) \quad (5)$$

was used for the calculation of f_{TF} . Here r is the interatomic distance and φ_0 the TF screening function.¹ Thus, this single calculation covers all

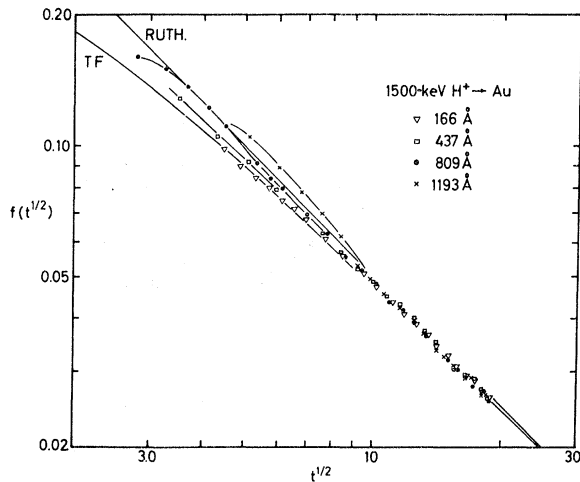


FIG. 2. Reduced scattering cross sections $f(t^{1/2}) dt = 2t^{3/2} \pi^{-1} a^{-2} d\sigma$ as a function of the product t of projectile energy and recoil energy; $t = \epsilon^2 \sin^2 \frac{1}{2}\vartheta$. The results are for 1.5-MeV $H^+ \rightarrow Au$. Deviations between data obtained on targets of different thicknesses are caused by multiple scattering. The Rutherford and the TF cross sections are shown as solid lines.

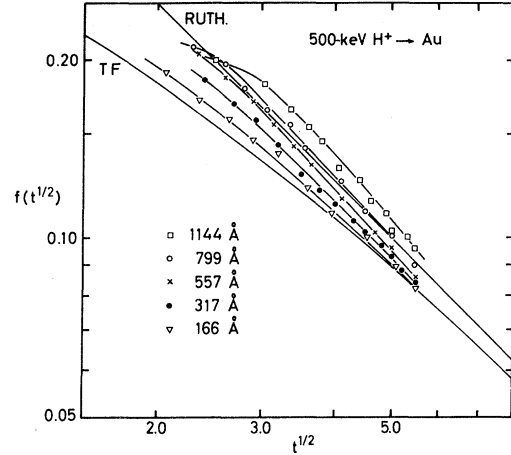


FIG. 3. Reduced cross sections for the scattering of 0.5-MeV H^+ on polycrystalline gold targets.

combinations of M_1 , Z_1 , M_2 , Z_2 , E , and ϑ . Note that Eq. (4) is exact for Rutherford scattering, where $f(t^{1/2}) = 1/(2t^{1/2})$. Figure 7 shows, together with our experimental data, f_{TF} as tabulated in Ref. 3 and the Rutherford value $f_R = 1/(2t^{1/2})$. It is seen from the figures that the region of interest in the present study is $0.4 < t^{1/2} < 25$. The calibration point corresponds to $t^{1/2} \approx 18$ as the Van de Graaff did not always run stably enough to allow a calibration at 2 MeV. At $t^{1/2} = 18$, $f_{TF} = 0.98 f_R$.

The calculations in Ref. 3 were only carried up to $t^{1/2} = 4$; for $t^{1/2} = 10$ and higher, the Rutherford values are given. We carried the computations of $f(t^{1/2})$ to higher values of $t^{1/2}$ than 4, using the same procedure as in Ref. 3. Thus our calculated values, which may best be seen from Fig. 8, replace the figures of Table 2a of Ref. 3 for $t^{1/2} > 4$.

IV. RESULTS AND DISCUSSION

Our raw data consist of tables of corresponding scattering angles and normalized yields Y in the transmission detector T . From the experimental parameters in question, we calculate $t^{1/2}$ and the yield $Y_R = Y_{R,0} \sigma_R / \sigma_{R,0}$ which we would have in the case of Rutherford scattering. Index 0 refers to the calibration point. Experimental values of $f(t^{1/2})$ are obtained as

$$f(t^{1/2}) = (Y/Y_R) f_R = Y/2t^{1/2} Y_R. \quad (6)$$

The energy entering the above-mentioned calculations is always $E = E_0 - \frac{1}{2} \Delta E$, where E_0 is the beam energy and ΔE the energy loss in the target foils. The accuracy of the stopping powers used to calculate ΔE is not critical. Possible errors disappear through the extrapolation to zero thickness. Figures 2-4 show $f(t^{1/2})$ obtained by this procedure for 1.5-MeV H^+ , 0.5-MeV He^+ , and 0.5-MeV Li^+ . These data have not been corrected for

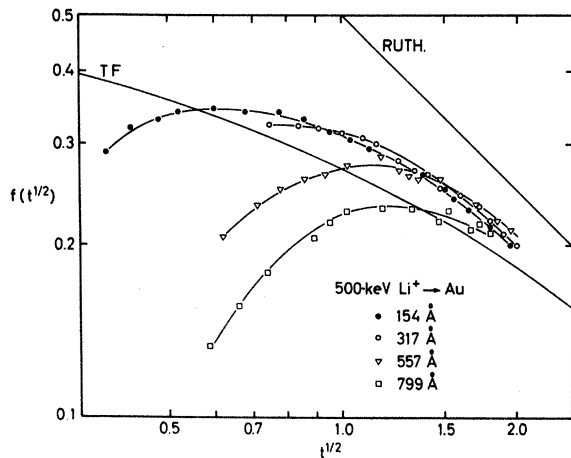


FIG. 4. Reduced scattering cross section for 0.5-MeV $\text{Li}^+ \rightarrow \text{Au}$. The data show very large multiple-scattering effects.

the influence of multiple scattering, and they are seen to depend systematically on foil thickness. The theoretical values are included for comparison. For $t^{1/2} > 10$, all data fall on top of each other. This confirms the earlier assumption that at $t^{1/2} = 18$, multiple scattering is of negligible influence for all foil thicknesses used here. For $t^{1/2} < 10$, the apparent value of $f(t^{1/2})$ is higher, the thicker the foil. This tendency is finally reversed for even smaller values of $t^{1/2}$.

Figures 5 and 6 show how the data from Figs. 3 and 4, respectively, are corrected for the influence of multiple scattering. For a fixed value of $t^{1/2}$ (and projectile and projectile energy), the data

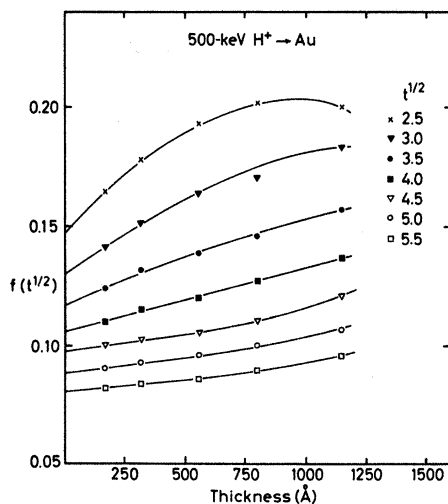


FIG. 5. Empirical correction for multiple-scattering effects performed on the raw data depicted in Fig. 3 (0.5-MeV $\text{H}^+ \rightarrow \text{Au}$). For a fixed value of $t^{1/2}$, the data are shown as a function of target thickness and extrapolation to zero thickness is performed.

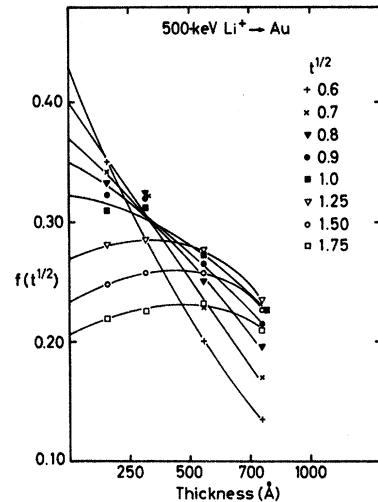


FIG. 6. Empirical corrections for multiple-scattering effects performed on the data of Fig. 4 (0.5-MeV $\text{Li}^+ \rightarrow \text{Au}$). The rather large extrapolations at small values of $t^{1/2}$ make the correction somewhat uncertain.

are depicted as a function of foil thickness. They usually lie on a smooth curve, and extrapolation is quite easy except at the lowest $t^{1/2}$ values. The extrapolation procedure is purely empirical. A gradual change of the shape of the extrapolation curves with changing $t^{1/2}$ is found. This is of considerable help when, for example, the extrapolations for low $t^{1/2}$ values in Fig. 6 are performed. Here evidence from all other measurements at corresponding $t^{1/2}$ are taken into account.

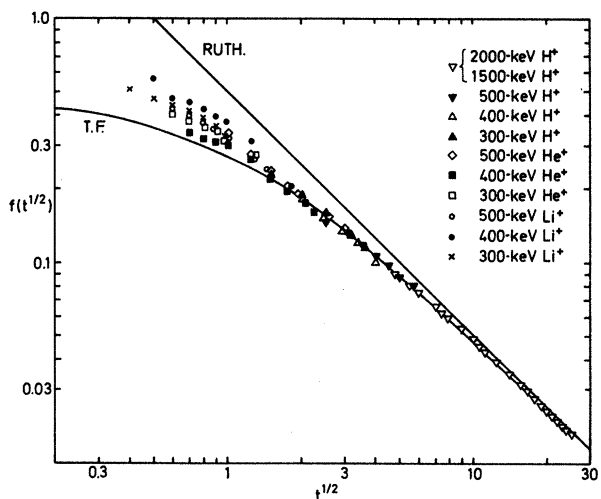


FIG. 7. Reduced scattering cross sections of gold for a large number of combinations of projectiles and projectile energies. All the data have been corrected for the influence of multiple scattering. With the possible exception of the lowest $t^{1/2}$ values, the points are seen to fall on a common curve.

The results of the extrapolation appear to be accurate to better than 5%, except at the lowest values of $t^{1/2} (\leq 1)$. The results for 300-, 400-, and 500-keV H^+ , He^+ , and Li^+ , together with 1500- and 2000-keV H^+ , are shown in Fig. 7. All H^+ and He^+ results scale, beyond doubt, to a common curve. The Li^+ data are perhaps slightly above the rest, but to a very good approximation, the scaling to a single curve is seen to be fulfilled.

Measurements of multiple-scattering distributions in gold with H^+ , He^+ , Li^+ , and several other ions did not show the scaling expected from the TF theory.¹⁰ Nor was this the case for distributions of Li^+ having passed through several target materials with $Z_2 \leq 32$, as measured by Schwabe and Stolle.¹¹ They noted that for fixed Z_1 and Z_2 , the discrepancy between calculated and measured angular distributions could be eliminated by simply choosing another screening parameter than that given by Eq. (3). This point of view is further elaborated by Meyer and Krygel,¹² who published tables to obtain experimental screening parameters from multiple-scattering data. For the results of Ref. 10, we may obtain a fit by choosing screening parameters smaller than those given by Eq. (3), the factors being 0.95 for H^+ and 0.63 for N^+ .

This raises the question of how accurately our data in Fig. 7 fix the screening parameter a . From Eqs. (1) and (2), $t^{1/2}$ is seen to be proportional to a , and consequently, the experimental values of $f(t^{1/2})$ are proportional to a^{-1} , as seen from Eq. (6). Changing a thus moves the experimental points along a line with slope -1 in Fig. 7. Hence, if the scattering is purely Rutherford, then the transformation is the identity as the Rutherford cross section does not depend on a . If the slope of the experimental curve at a given point is $-(1-\alpha)$, then a relative change of the screening parameter of $\beta = \delta a/a$ will move the curve a vertical distance corresponding to $\delta f/f = \beta\alpha$ with respect to the untransformed curve. This is seen to fix the screening parameter for both H^+ and He^+ to Eq. (3) to a factor of $1.00^{+0.10}_{-0.05}$. Furthermore, the Li^+ results, partly falling in a $t^{1/2}$ region where they are more sensitive to change in the screening parameter, are seen to scale together with He^+ within a factor of 1.10 ± 0.10 . This is certainly in disagreement with the scaling factors obtained from our multiple-scattering results¹⁰ as given at the end of the preceding paragraph. The experiments of Ref. 10 were, in part, performed with the very same target as those used here. We propose that at the $t^{1/2}$ values mainly responsible for multiple scattering (lower than the lowest values treated here), the scaling breaks down, but this breakdown may not be removed over the entire $t^{1/2}$ region by a simple change of a . This disagrees with the above-

mentioned assumption of Refs. 11 and 12, but in the light of the peak structure found by Loftager⁴ in $f(t^{1/2})$ at lower values of $t^{1/2}$, the result is not surprising.

Finally, Fig. 8 shows our results if we accept all data of Fig. 7 as being statistically scattered around a common curve and calculate their weighted mean. As the assumption apparently does not hold too well for Li^+ , a hump is seen in the results around $t^{1/2} = 1$, where Li^+ begins to strongly influence the mean. Unfortunately, the overlap between Li^+ and He^+ is not large enough for us to see whether this is evidence of a small peak in $f(t^{1/2})$ of the same type as those found by Loftager.⁴ The figure also displays the result of our accurate computation of the theoretical cross section mentioned in Sec. III. Above $t^{1/2} = 1.5$, the agreement between experiment and theory is satisfactory. Below this value of $t^{1/2}$, the experimental values are higher than those found theoretically.

Our results may also be compared to those from Refs. 4-6. Loftager and Clausen⁴ used gaseous targets. Results for 500-keV $He^+ \rightarrow He$, 500-keV $Ne^+ \rightarrow Ne$, and 500-keV $He^+ \rightarrow Ar$ lie within the region of interest. For $t^{1/2} > 1$, they all agree with the theoretical curve and thus with our results for $t^{1/2} < 1.5$. For $t^{1/2} < 1$, they are lower than the theoretical results and peak structures are observed. van Wijngaarden *et al.*⁵ also used gold targets. They irradiated with 30-110-keV H^+ , He^+ , Li^+ , and B^+ ions, but much larger scattering angles placed the results within our $t^{1/2}$ region. Their results are shown in Fig. 8. They agree with ours, but the scatter is larger. As previously mentioned, they did not analyze their data in terms of $f(t^{1/2})$ and thus could not compare the results for different ions.

Taylor *et al.*⁶ used gaseous targets. Within their

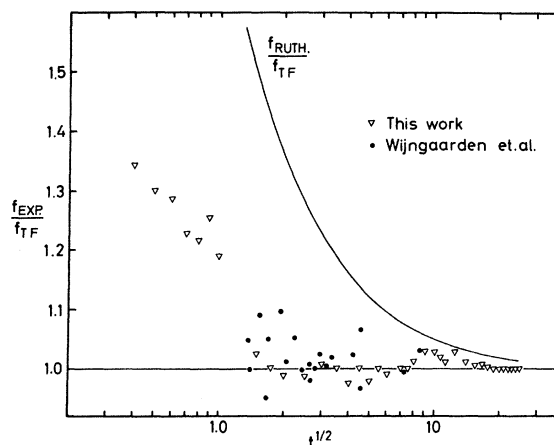


FIG. 8. Weighted mean of the results of Fig. 7 normalized to the TF cross section. This figure also shows the ratio between the Rutherford and the TF cross sections for large values of $t^{1/2}$.

accuracy, their results agree with ours, but their 208-keV $\text{He}^+ \rightarrow \text{Ar}$ and 418-keV $\text{He}^+ \rightarrow \text{Ar}$ results only scale together in the $f(t^{1/2})$ diagram to within 20%.

V. CONCLUSIONS

It was found possible to investigate scattering cross sections in the weakly screened Rutherford region by means of solid targets, provided an em-

pirical multiple-scattering correction was performed. The results show that the TF scaling was well fulfilled for H^+ , He^+ , and Li^+ on gold, in contrast to the case of multiple scattering.¹¹ The numerical values of the cross sections agree with those expected from the TF theory as well as with existing experimental results by several authors, mainly obtained on gaseous targets.

¹P. Gombas, *Die statistische Theorie des Atoms und ihre Anwendungen* (Springer-Verlag, Wien, 1949).

²N. Bohr, Kgl. Danske Videnskab. Selskab, Mat.-Fys. Medd. **18**, No. 8 (1948).

³J. Lindhard, V. Nielsen, and M. Scharff, Kgl. Danske Videnskab. Selskab, Mat.-Fys. Medd. **36**, No. 10 (1968).

⁴P. Loftager and G. Claussen, *Second International Conference on the Physics and Electronics of Atomic Collisions* (MIT Press, Boston, 1969), p. 518; also P. Loftager (private communication).

⁵A. van Wijngaarden, E. S. Brimmer, and W. E. Baylis, Can. J. Phys. **48**, 1835 (1970).

⁶G. O. Taylor, E. W. Thomas, and D. W. Martin,

Phys. Rev. A **2**, 85 (1970).

⁷P. Sigmund, Phys. Rev. **184**, 383 (1969).

⁸H. E. Schiøtt and P. V. Thomsen, Rad. Effects **14**, 39 (1972).

⁹H. H. Andersen and J. Bøttiger, Phys. Rev. B **4**, 2105 (1971).

¹⁰H. H. Andersen, J. Bøttiger, and H. Knudsen, Rad. Effects **13**, 203 (1972).

¹¹S. Schwabe and R. Stolle, Phys. Status Solidi (b) **47**, 111 (1971).

¹²L. Meyer and P. Krygel, Nucl. Instr. Methods **98**, 381 (1972).

Equilibrium Charge-State Distributions of 2–15-MeV Tantalum and Uranium Ions Stripped in Gases and Solids*

Andrew B. Wittkower[†]

High Voltage Engineering Corporation, Burlington, Massachusetts 01803

and

Hans D. Betz

Department of Physics, Laboratory for Nuclear Science, Massachusetts Institute of Technology, Cambridge, Massachusetts 03139

(Received 6 April 1972)

Equilibrium charge-state fractions have been measured for tantalum and uranium ions with energies of 2, 4, 6, 8, 10, and 15 MeV, stripped in H_2 , He, N_2 , O_2 , Ar, Kr, Xe, carbon, and gold. Average charge and form of the charge distributions and the dependence on ion velocity and target species are discussed. The results on the average charge are compared with theoretical and semiempirical predictions. An anomaly has been found in the particular case of helium targets in which certain charge-state fractions are of unusual magnitude, leading to a relatively high average charge.

INTRODUCTION

The charge of a fast ion moving through matter fluctuates as a result of electron loss and capture in collisions with the stationary atoms of the target. After a sufficient number of collisions an equilibrium distribution of charges is established which is dependent only on the velocity of the ions and the nature of the target. In the present experiments, equilibrium charge-state distributions have been measured for mass-181 tantalum ions and mass-238 uranium ions, having energies between 2 and 15 MeV, traversing targets of hydrogen, helium, nitrogen, oxygen, argon, krypton, and xenon

gases, and foils of carbon and gold. Typical parts of our results on uranium ions have already been reported¹; no previous measurements of equilibrium charge-state distribution had been published for either projectile species in any target material. Beams of uranium ions have been accelerated first by the group at Heidelberg, but only the results on the average charge have been published.² Similarly, the groups at Burlington and Cambridge (Massachusetts) reported average charge states of tantalum and uranium ions emerging from carbon foils.³ Most recently, the group at Oak Ridge communicated some equilibrium charge-state distributions of uranium ions.⁴